J Mater Sci (2008) 43:6081–6086
DOI 10.1007/s10853-008-2953-y

Coupling kinetic dislocation model and Monte Carlo algorithm for recrystallized microstructure modeling of severely deformed copper

M. Kazeminezhad · E. Hosseini

Received: 12 June 2008 / Accepted: 14 August 2008 / Published online: 4 September 2008

Abstract By coupling a kinetic dislocation model and Monte Carlo algorithm, the recrystallized microstructure of severely deformed Oxygen Free High Conductivity Copper (OFHC) is predicted at different strains imposed by Equal-Channel-Angular-Pressing (ECAP) and annealing temperatures. From a flow field model, the strain rate distribution during the ECAP of the material in a curved die is calculated. Then using the kinetic dislocation model, the total dislocation density and correspondingly the stored energy after each ECAP pass is estimated. Utilizing the Monte Carlo algorithm and the stored energy, the recrystallized microstructure is predicted. The results show that the recrystallized grain size is decreased rapidly from the strain of first to fourth pass and then it is decreased slowly. Also, it is achieved that with increasing the annealing temperature, the grain size is increased. Moreover, a good agreement is observed between the predicted results and experimental data.

Introduction

Severe plastic deformation makes metals with high-dislocation density. The dislocations form as a cell structure [1–3]. Annealing process on severely deformed metals has a great importance since it leads to a fine grained microstructure due to occurrence of recrystallization. The fine grained microstructure has novel properties such as high strength and super plasticity [4, 5]. Thus, recrystallized microstructure modeling of severe plastic deformation of materials can help to find a proper annealing process and achieve a desirable microstructure and properties. Due to complexity of dislocation structure in severely deformed materials and more unknown phenomenon in their annealing process, a limit works can be found on modeling of their recrystallized microstructure. Recently, the first author has presented an approach for predicting the microstructure of copper after Equal-Channel-Angular-Pressing (ECAP) and annealing [6]. ECAP is one of the most popular methods of imposing bulk severe plastic deformation to materials [1–3]. It involves the use of a die that contains two intersecting channels of equal cross-section, where the sample cross-section remains unchanged during processing and the imposed plastic deformation to the sample includes a pure shear. In the recent work [6], using a simple analytical relationship the strain was calculated. Then the subgrain size and stored energy due to the deformation were estimated from the achieved strain utilizing empirical relationships. The stored energy was input to the Monte Carlo algorithm and the recrystallized grain sizes were simulated at different pass numbers of ECAP and annealing temperatures. However, a good agreement was achieved between the modeling results and experimental data, some errors of prediction were seen in some cases. This can be attributed to the consideration of simple analytical relationship in calculation of strain and empirical relationships in estimation of subgrain size and stored energy. Thus, in this study a new idea is used to improve the modeling results and decrease the errors of prediction. The idea includes coupling of kinetic dislocation model and Monte Carlo algorithm [7–11]. However, these models have been individually used before to predict the microstructure evolution of materials. The advantage of the coupling is that the kinetic dislocation model can consider the complex structure of dislocation cells and predicts an exact value of total

M. Kazeminezhad (✉) · E. Hosseini
Department of Materials Science and Engineering, Sharif University of Technology, Azadi Avenue, Tehran, Iran
e-mail: mkazemi@sharif.edu

dislocation density from which the stored energy can be calculated. Then, to simulate the recrystallized microstructure of severely deformed copper, the stored energy is input to the Monte Carlo algorithm. It should be mentioned that the kinetic dislocation model depends on strain rate [7–9]. Thus, an exact value of strain rate should be input to the kinetic dislocation model. To do so, the flow field model, presented by Tóth et al. [12, 13], for sharp ECAP die is developed for a curved ECAP die studied in the present work. The material studied in this research is Oxygen Free High Conductivity Copper (OFHC).

Kinetic dislocation model

In this section, the kinetic dislocation model used for estimating the stored energy due to severe plastic deformation is described. In three dimensional version of this model, it is assumed that the dislocation structure of the severely deformed materials formed as cell is composed of two regions. The first one is cell walls and the second one is cell interiors, where the dislocation densities are ρ_w and ρ_c, respectively. The evolution of dislocation densities with time of deformation can be expressed by the following equations [7–9]

$$\frac{\mathrm{d}\rho_w}{\mathrm{d}t} = \frac{6\beta^*\dot{\gamma}_c(1-f)^{2/3}}{bdf} + \frac{\sqrt{3}\beta^*\dot{\gamma}_c(1-f)\sqrt{\rho_w}}{fb} - k_0\dot{\gamma}_w\rho_w\left(\frac{\dot{\gamma}_w}{\dot{\gamma}_0}\right)^{\frac{-1}{n_w}} \quad (1)$$

$$\frac{\mathrm{d}\rho_c}{\mathrm{d}t} = \frac{\alpha^*\dot{\gamma}_w\sqrt{\rho_w}}{\sqrt{3}b} - \frac{6\beta^*\dot{\gamma}_c}{bd(1-f)^{1/3}} - k_0\dot{\gamma}_c\rho_c\left(\frac{\dot{\gamma}_c}{\dot{\gamma}_0}\right)^{\frac{-1}{n_c}} \quad (2)$$

where, t is the time of process, $\dot{\gamma}_c$ is the resolved shear strain rate in the cell interiors, $\dot{\gamma}_w$ is the resolved shear strain rate in the cell walls, $\dot{\gamma}_0$ is the reference shear strain rate, b is the Burgers vector length, f is the volume fraction of the cell walls, d is the cell size. The parameters $\alpha^*$and β^* denote the fraction of operative Frank-Read sources and a fraction of dislocations which are within a certain distance from a wall will be woven into the wall, respectively. The value of k_0 is the coefficient of recovery in the cell walls and cell interiors, and the values of n_w and n_c are their exponents of recovery, respectively. The exponents characterize the strain rate sensitivity of dislocations annihilation process.

In the above-mentioned equations, the volume fraction of the cell walls depends on the strain [7]:

$$f = f_\infty + (f_0 - f_\infty)\exp(-\lambda_f\gamma_r) \quad (3)$$

where f_0 is the initial volume fraction of the cell walls, f_∞ is the saturated magnitude of the cell walls volume fraction, γ_r is the resolved shear strain and λ_f is a numerical constant.

It has been reported that the cell size can be calculated from [7]:

$$d = K\rho_{\text{total}}^{-0.5} \quad (4)$$

where K is the proportionality constant and ρ_{total} is the total dislocation density.

The total dislocation density can be determined as [7]:

$$\rho_{\text{total}} = f\rho_w + (1-f)\rho_c \quad (5)$$

To make the strain compatibility along the cell interiors and cell walls, it is assumed that [7]:

$$\dot{\gamma}_c = \dot{\gamma}_w = \dot{\gamma}_r \quad (6)$$

where $\dot{\gamma}_r$ is the resolved shear strain rate. Considering the Taylor assumption, the resolved shear strain rate can be calculated from equivalent Von-Mises strain rate.

As can be seen the described model is dependent on the strain rate of deformation. Thus to achieve the strain rate, a mechanical model is required. Since, in this research the ECAP process with curved die is studied, to do so a flow field model proposed in the prior works for a sharp die is developed for a curved die.

Flow field model for curved die

The flow field model presented by Tóth et al. [12, 13] for a 90° ECAP die is developed for a curved die studied here, see Fig. 1. At first, a brief description on the flow field model is presented. The following analytical function can

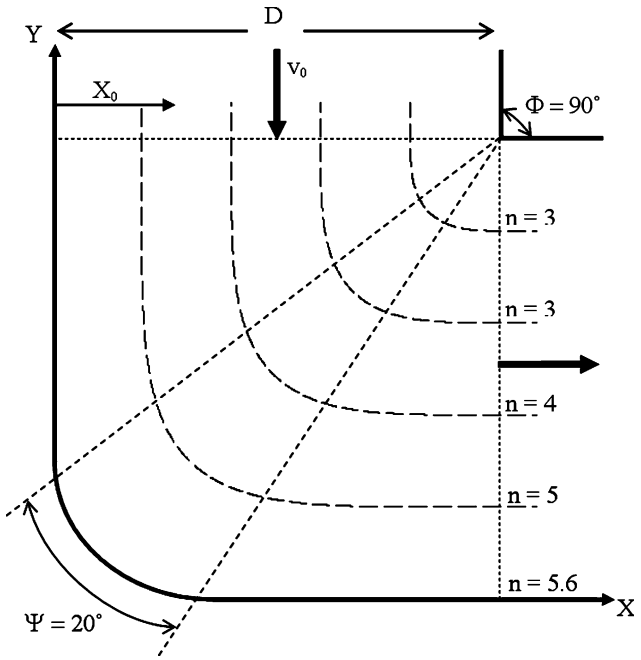

Fig. 1 Illustration of equal-channel-angular-pressing process and flow lines (D = 25 mm and v_0 = 2.5 mm/s)

determine the flow line of material through ECAP die in a good agreement with finite element analysis:

$$\Omega = (D-x)^n + (D-y)^n = (D-x_0)^n \tag{7}$$

where D is the die diameter, x and y are the coordinates, n is the shape parameter of flow line, x_0 denotes the position of flow line from the outer wall of die.

In prior works, it has been reported that the maximum n value is theoretically ∞ for a material passing through a 90° die if no dead zone formation is assumed. Indeed, the mentioned n value is related to the outer wall of die. If the dead zone formation is assumed, the maximum value of n is dependent on the die diameter [14]. Since in this study the outer wall of die has a curvature at the intersecting position of the channels and the formation of dead zone does not occur [14], the upper bound of n value is limited by an n value calculated for the geometry of the outer wall. On the other hand, it depends on the magnitude of die curvature. Considering the geometry of the studied die, the n value of outer wall is achieved 5.6. Thus, the n values are assumed to be lied between 3 and 5.

From the mentioned flow function, the velocity field can be computed as follows [12, 13]:

$$v_x = v_0\left(\frac{D-y}{D-x_0}\right)^{n-1} \tag{8}$$

$$v_y = -v_0\left(\frac{D-x}{D-x_0}\right)^{n-1} \tag{9}$$

where v_0 is the ram speed.

The velocity gradient is analytically obtained from the velocity field [12, 13]:

$$L_{xx} = \frac{\partial v_x}{\partial x} = -v_0(1-n)(D-x)^{n-1}(D-y)^{n-1}(D-x_0)^{1-2n} \tag{10}$$

$$L_{yy} = \frac{\partial v_y}{\partial y} = v_0(1-n)(D-x)^{n-1}(D-y)^{n-1}(D-x_0)^{1-2n} \tag{11}$$

$$L_{xy} = \frac{\partial v_x}{\partial y} = v_0(1-n)(D-x)^{n}(D-y)^{n-2}(D-x_0)^{1-2n} \tag{12}$$

$$L_{yx} = \frac{\partial v_y}{\partial x} = -v_0(1-n)(D-y)^{n}(D-x)^{n-2}(D-x_0)^{1-2n} \tag{13}$$

The strain rate tensor is the symmetrical part of the velocity gradient. Thus, from the above equations the Von-Mises equivalent strain rate can be calculated. Then, an integration of the Von-Mises strain rate along the flow line gives the total Von-Mises strain in one pass:

$$\varepsilon_{\text{Von-Mises}} = \int \left[\frac{n-1}{\sqrt{3}} v_0 (D-x_0)^{1-2n}(D-x)^{n-2} (D-y)^{n-2}\left[(D-x)^2 + (D-y)^2\right]\right] \mathrm{d}t \tag{14}$$

Monte Carlo algorithm

The Monte Carlo algorithm used in this work is based on the works carried out by Srolovitz et al. [10, 11] for recrystallization. However, a new nucleation model is utilized here.

At first, the stored energy due to severe plastic deformation is calculated from the total dislocation density estimated from the kinetic dislocation model. The stored energy due to deformation is equal to $0.5Gb^2\rho_{\text{total}}$ [15], where G is the shear modulus. Then, the stored energy is mapped on the triangular lattice, i.e., the stored energy is assigned to each lattice site, which has a random integer orientation between 1 and 48 [10, 11]. In the recent work of the first author, it has been concluded that a constant nucleation rate is prevailed during recrystallization of severely deformed copper [6]. Since the stored energy and annealing temperature are controlled the nucleation rate, the following constant nucleation rate model presented by other researchers is used [16, 17]:

$$\dot{N} = Z(H_\Omega(t) - H_{\text{Min}}(t))\ V_\Omega(t)\ \exp\left(\frac{-Q_N}{k_B T}\right) \tag{15}$$

where Z is a constant which sets the order of 10^{-2} for the fraction of nucleus density on the lattice, $H_\Omega(t)$ is the stored energy due to deformation, $H_{\text{Min}}(t)$ is the minimum stored energy due to deformation needed for recrystallization, $V_\Omega(t)$ is the fraction of material for which nucleation is still possible at time t, k_B is the Boltzmann's constant, Q_N is the activation energy for nucleation, T is the absolute temperature.

Since the minimum strain leads to recrystallization is approximately 3% [15] and the strain in ECAP is large, therefore $H_{\text{Min}}(t)$ in the above equation is ignorable in compared with $H_\Omega(t)$. Under isothermal heat treatment, the average nucleation rate is dependent only on the stored energy. Thus, the present simulation does not use the time-dependent values of stored energy.

It is worth mentioning that due to high stored energy one lattice site is considered as the critical size of the nucleus by assigning the random integer orientation between 48 and 64 [10, 11].

In the Monte Carlo algorithm the microstructure evolution is modeled by reorienting attempts of each randomly chosen lattice site to the new random orientation of one of its nearest neighbors [10]. These attempts are tracked by

calculating the changes in the energy of system. This energy includes the grain boundary energy and stored energy, expressed as follows [10, 11, 18–20]:

$$E_i = \sum_{i=1}^{N} H_i\, g(S_i) + \frac{1}{2}\sum_{i=1}^{N_i}\sum_{j=1}^{N_j} \gamma_{ij} \qquad (16)$$

where H_i is the stored energy due to deformation at lattice site i, γ_{ij} is the grain boundary energy between two neighboring lattice sites i and j, S_i is the orientation of site i, $g(S_i)$ is the step function that is unity for unrecrystallized site and zero for recrystallized site, N_i is the total number of lattice sites, N_j is the number of nearest neighbors of site i. In triangular lattice N_j is equal to 6.

If the change in energy of system due to the reorientation is less than or equal to zero, the reorientation is accepted and if not the orientation of the site should remain as before. It should be noted that all reorientations of the recrystallized sites to the unrecrystallized ones are not acceptable. The reorientations of unrecrystallized site to the orientation of the neighboring unrecrystallized site are considered as recovery due to subgrain growth [19, 20]. If the recrystallized site reorients to the neighboring recrystallized site, the process represents the grain growth phenomenon after recrystallization.

Results and discussion

Considering the procedure mentioned in prior sections, a computer code is developed to simulate the microstructure. It should be noted that the ECAP process is carried out through route C (i.e., 180° rotation of billet between two passes) where the strain states and magnitudes on the top and bottom of billet are approximately the same. Since, in the literature the main data can be found for the cross section and not for each point at the cross section of billet, thus in this study the calculated data are the mean values at the cross section. As seen in Fig. 2, the Von-Mises strain during each pass of ECAP process is increased with different slopes. This phenomenon is related to the variation of the strain rate during the passage of the material in the plastic zone. In the flow field model, zero strain rate is predicted when the material enters to the working part of the die and it is increased to a maximum value at the intersecting plane of the die channels. Thus, at the primary section of die the strain accumulation in material is small and it is increased rapidly by closing to the intersecting plane. When the material passes from the plane, i.e., the position of maximum strain rate, the strain rate is decreased down to zero where the material exits from the working part of the die. Therefore, the strain is increased slowly. In the next pass, this trend is repeated. It should be noted that this trend is similar to that achieved by the fan model [21].

In Fig. 3, the fraction of cell walls, which are the incidental dislocation boundaries (IDBs), is presented versus pass number. As can be seen, the fraction is decreased with increasing the pass number. This trend is in agreement with the experimental results presented by McKenzie et al. [9] and shows although the surface of cell walls grows as strain accumulates, but the cell walls become increasingly thin. Thus, the volume fraction of cell walls is decreased [22–24].

Considering the given constants in Table 1, the cell walls, cell interiors, and total dislocation densities after each pass of ECAP are calculated. In Fig. 4, the dislocation densities are plotted versus Von-Mises strain of each pass. The total dislocation density is increased rapidly from the first to fourth pass and in following passes it is increased with a lower rate. The presented results are consistent with the data presented before [26].

To predict the recrystallized grain size of severely deformed OFHC, at first the stored energy in each pass is calculated from the total dislocation density. Then by inputting the stored energy to the described Monte Carlo algorithm, the recrystallized grain size of the material is achieved versus the Von-Mises strain at a specific annealing temperature. As it is presented in Fig. 5, the

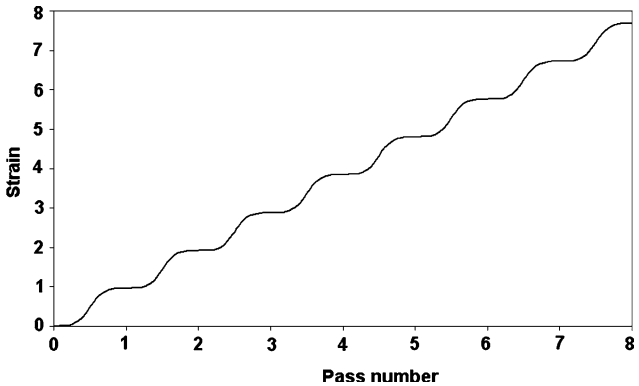

Fig. 2 The Von-Mises strain versus pass number

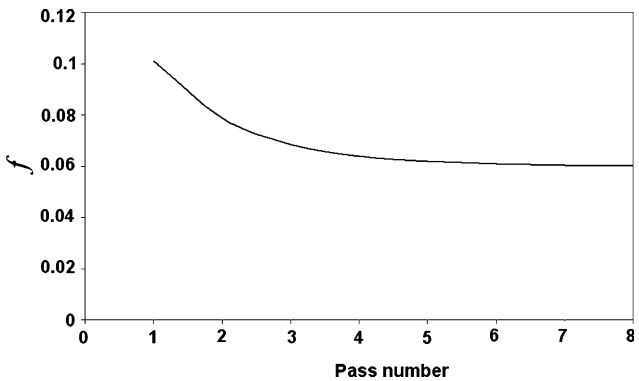

Fig. 3 The fraction of cell walls versus pass number

Table 1 The values of parameters and constants used in the model [7, 9, 12, 13, 15–17, 25]

Symbol	Value
α^*	0.02
β^*	0.01
$\dot{\gamma}_0$	1 s^{-1}
b	2.56 × 10^{-10} m
ρ_{c_0}	10^{13} m^{-2}
ρ_{w_0}	10^{14} m^{-2}
k_0	2.3
n_c	50
n_w	4
K	10
f	0.25
f_∞	0.06
λ_f	0.31
G	42.1 GPa
Q_N	24 kcal/gm-atom
k_B	1.38 × 10^{-23} J/degree
γ_{ij}	0.625 Jm^{-2}

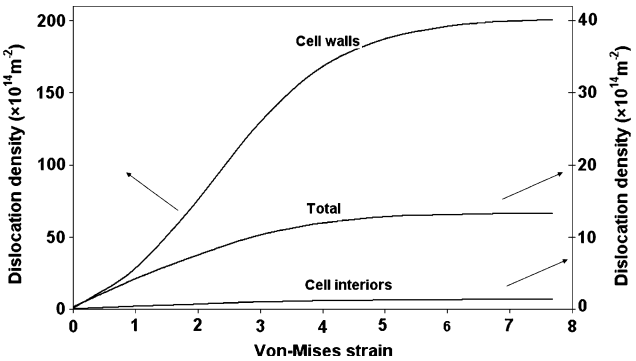

Fig. 4 The effect of Von-Mises strain on the dislocation densities

recrystallized grain size is decreased rapidly from the strain of first to fourth pass and then it is decreased slowly. This is attributed to the changes of the total dislocation density mentioned before, which is the driving force of nucleation phenomenon during recrystallization. With increasing the dislocation density, the nucleation rate is increased and finally it leads to the formation of the smaller grain size. As can be seen in the figure, a good agreement is found between the modeling results and experimental data [27]. Also, the grain sizes of the OFHC after 4 and 6 ECAP passes are predicted at different annealing temperature. The predicted grain sizes are presented in Fig. 6. As can be observed, the grain sizes are increased with increasing the annealing temperature. Also, Fig. 6 shows that the predicted grain sizes are consistent well with the experimental data [28–30]. However, with increasing the temperature the

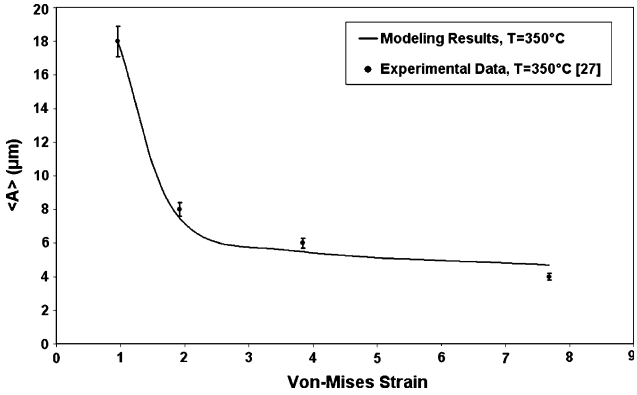

Fig. 5 The effect of Von-Mises strain on the recrystallized grain size (Annealing temperature = 350 °C, Annealing time = 1 h), symbol <A> on *y*-axis shows the mean grain diameter after annealing

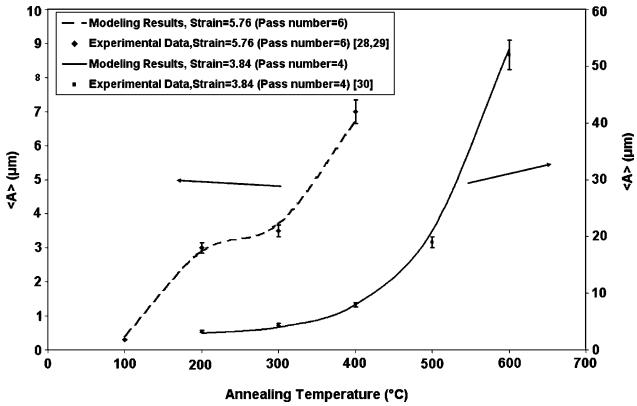

Fig. 6 The effect of annealing temperature on the recrystallized grain size at different pass numbers (Annealing time = 1 h), symbol <A> on *y*-axis shows the mean grain diameter after annealing

nucleation rate is increased, the kinetics of grain growth is increased and finally the higher annealing temperature leads to the coarser grain size.

It should be noted that in this study by utilizing the kinetic dislocation model for calculating the total dislocation density as well as stored energy in each ECAP pass, the errors in predicting the recrystallized grain size is smaller than that in the prior work.

Conclusions

In this study, the recrystallized microstructure modeling of the OFHC after ECAP is carried out. To do so, a flow filed model, kinetic dislocation model, and Monte Carlo algorithm are utilized. The following conclusions can be presented:

1. A good agreement is achieved between the modeling results and experimental data. Also in the present

work, the errors in predicting the recrystallized grain size are smaller than that in the prior work.
2. The Von-Mises strain during each pass of ECAP process is increased with different slopes.
3. The total dislocation density is increased rapidly from the first to fourth pass and in following passes it is increased with a lower rate.
4. The recrystallized grain size is decreased rapidly from the strain of first to fourth pass and then it is decreased slowly.
5. However, with increasing the temperature the nucleation rate is increased, the kinetics of grain growth is increased and finally the higher annealing temperature leads to the coarser grain size.

Acknowledgement The authors wish to thank the research board of Sharif University of Technology for the financial support and the provision of the research facilities used for this work.

References

1. Valiev RZ, Langdon TG (2006) Prog Mater Sci 51:881. doi:10.1016/j.pmatsci.2006.02.003
2. Zhao G, Xu S, Luan Y, Guan Y, Lun N, Ren X (2006) Mater Sci Eng 437A:437
3. Fukuda Y, Oh-ishi K, Furukawa M, Horita Z, Langdon TG (2007) J Mater Sci 42:1501. doi:10.1007/s10853-006-0753-9
4. Dalla Torre F, Lapovok R, Sandlin J, Thomson PF, Davies CHJ, Pereloma EV (2004) Acta Mater 52:4819. doi:10.1016/j.actamat.2004.06.040
5. Yu CY, Sun PL, Kao PW, Chang CP (2004) Mater Sci Eng 366A:310
6. Kazeminezhad M (2008) Comput Mater Sci 43:309
7. Estrin Y, Toth LS, Molinari A, Brechet Y (1998) Acta Mater 46:5509. doi:10.1016/S1359-6454(98)00196-7
8. Toth LS, Molinari A, Estrin Y (2002) J Eng Mater Technol 124:71. doi:10.1115/1.1421350
9. Mckenzie PWJ, Lapovok R, Estrin Y (2007) Acta Mater 55:2985. doi:10.1016/j.actamat.2006.12.038
10. Srolovitz DJ, Grest GS, Anderson MP (1986) Acta Metall 34:1833. doi:10.1016/0001-6160(86)90128-8
11. Srolovitz D, Grest G, Anderson M, Rollett A (1988) Acta Metall 36:3115. doi:10.1016/0001-6160(88)90313-6
12. Toth LS, Massion RA, Germain L, Baik SC, Suwas S (2004) Acta Mater 52:1885. doi:10.1016/j.actamat.2003.12.027
13. Toth LS (2005) Comput Mater Sci 32:568. doi:10.1016/j.commatsci.2004.09.007
14. Stoica GM, Fielden DE, McDaniels R, Liub Y, Huangb B, Liaw PK et al (2005) Mater Sci Eng 410A:239
15. Humphreys FJ, Hatherly M (2004) Recrystallization and related annealing phenomena. Elsevier, Oxford
16. Ivasishin OM, Shevchenko SV, Vasiliev NL, Semiatin SL (2006) Mater Sci Eng 433A:216
17. Byrne JG (1965) Recovery recrystallization and grain growth. Mcmillan Company, USA
18. Seo YS, Chun YB, Hwang SK (2008) Comput Mater Sci 43:512
19. Song X, Rettenmayr M, Muller C, Exner HE (2001) Metall Mater Trans 32A:2199
20. Song X, Rettenmayr M (2002) Mater Sci Eng 332A:153
21. Beyerlein IJ, Tome CN (2004) Mater Sci Eng 380A:171
22. Enikeev NA, Kimb HS, Alexandrov IV (2007) Mater Sci Eng A 460–461:619. doi:10.1016/j.msea.2007.02.005
23. Mecking H, Kocks U (1981) Acta Mater 29:1865. doi:10.1016/0001-6160(81)90112-7
24. Estrin Y, Mecking H (1984) Acta Mater 32:57. doi:10.1016/0001-6160(84)90202-5
25. Baik SC, Estrin Y, Kim HS, Hellmig RJ (2003) Mater Sci Eng A 351:86. doi:10.1016/S0921-5093(02)00847-X
26. Mishra A, Kad BK, Gregori F, Meyers MA (2007) Acta Mater 55:13. doi:10.1016/j.actamat.2006.07.008
27. Kadri SJ, Hartwig KT (2006) Mater Sci Forum 503:349
28. Neishi K, Horita Z, Langdon TG (2002) Mater Sci Eng 325A:54
29. Neishi K, Horita Z, Langdon TG (2003) Mater Sci Eng 352A:129
30. Flinn JE, Field DP, Korth GE, Lillo TM, Macheret J (2001) Acta Mater 49:2065. doi:10.1016/S1359-6454(01)00102-1